Erciyes Med J 2017; 39(3): 125-30 • DOI: 10.5152/etd.2017.17033

Diffusion-Weighted Imaging of the Parotid Gland: Can the Apparent Diffusion Coefficient Discriminate Between Normal and Abnormal Parotid Gland Tissues?

ORIGINAL INVESTIGATION

Ayman Mohamed Abdel Mottelb Aly Nada[1], Ayda Aly Youssef[1], Ayman Abdel Hamid El Basmy[2], Ayman Abdel Wahab Amin[1], Ahmed Mohamed Shokry[1]

ABSTRACT

Objective: This study attempted to investigate the importance of diffusion weighted (DW)-echo planar imaging (EPI) in the characterization of normal parotid glands to facilitate the early detection of abnormal changes.

Materials and Methods: This study was conducted between July 2014 and January 2016. Seventy-three patients were assessed by conventional and diffusion weighted Magnetic Resonance Imaging (MRI). Diffusion weighted MRI was performed by a single-shot spin echo (SE) echo planar imaging (EPI) sequence using b-values of 0, 500, and 1000. The Apparent Diffusion Coefficient (ADC) was automatically generated on the operating console.

Results: The mean apparent diffusion coefficients (ADCs) ±SD of the superficial lobes were $0.89\times10^{-3}\pm0.2\times10^{-3}$ and $0.9\times10^{-3}\pm0.17\times10^{-3}$ mm²/s in the right and left sides, respectively. The mean ADCs of the deep lobes were $1.02\times10^{-3}\pm0.27\times10^{-3}$ and $0.97\times10^{-3}\pm0.27\times10^{-3}$ mm²/s in the right and left sides, respectively. The mean ADCs of the deep lobes were $1.02\times10^{-3}\pm0.27\times10^{-3}$ and $0.97\times10^{-3}\pm0.27\times10^{-3}$ mm²/s in the right and left sides, respectively. The mean±SD ADC of a normal parotid gland was $1.12\times10^{-3}\pm0.12\times10^{-3}$ mm²/s. The mean±SD ADCs of benign and malignant tumors were $1.16\times10^{-3}\pm0.31\times10^{-3}$ mm²/s and 0.82×10^{-3} mm²/s, respectively.

Conclusion: The evaluation of the morphological characteristics of the parotid glands along with the Diffusion-weighted imaging (DWI) signal and ADC measurement may be valuable for detecting early pathological changes

Keywords: Magnetic resonance imaging , parotid glands, diffusion weighted imaging , apparent diffusion coefficient

Cite this article as: Aly Nada AMAM, Aly Nada A, El Basmy AAH, Amin AAW, Shokry AM. Diffusion-Weighted Imaging of the Parotid Gland: Can the Apparent Diffusion Coefficient Discriminate Between Normal and Abnormal Parotid Gland Tissues? Erciyes Med J 2017; 39: 125-30.

[1]Department of Diagnostic and Interventional Radiology, National Cancer Institute, Cairo University, Egypt

[2]Department of Diagnostic and Interventional Radiology, Al Kasr Al Ainy medical school, Cairo University, Egypt

Submitted 11.02.2017

Accepted 10.04.2017

Correspondence Ayman Mohamed Abdel Mottelb Aly Nada, Department of Diagnostic and Interventional Radiology, National Cancer Institute, Cairo University, Egypt

Phone: 00201006312828
e.mail: amn_med09@hotmail.com

INTRODUCTION

A broad spectrum of pathological conditions can affect the parotid glands. However, although unilateral parotid lesions are more frequently seen, bilateral parotid lesions are not uncommon (1).

Parotid swelling can result from a diverse spectrum of pathologies: inflammation or infections [e.g., bacterial, viral (e.g., mumps or HIV sialopathy), or chronic sialadenitis], autoimmune diseases (e.g., Sjogren's disease and chronic recurrent parotitis), granulomatous diseases (e.g., Wegener's granulomatosis and sarcoidosis), Kimura's disease, miscellaneous diseases (e.g., sialadenosis, polycystic disease, radiation sialadenitis, and pneumoparotid), neoplastic diseases (e.g., pleomorphic adenoma, Warthin's tumor, and mucosa-associated lymphoid tissue lymphoma), and pseudolesions (e.g., hypertrophy of the masseter muscle) (2).

The general evaluation of parotid lesions includes the so-called triple assessment, which refers to clinical examination, imaging, and biopsy (3).

Due to selection bias, fine needle aspiration cytology (FNAC) is not always conclusive. FNAC cannot be performed if the lesion is located in the deep lobe. Therefore, preoperative imaging plays a major role in the discrimination of inflammatory conditions from neoplastic conditions as well as in the differentiation between benign and malignant neoplasms; therefore, surgical planning is valuable in such cases. Few clinical symptoms, such as facial nerve palsy, allow the diagnosis of malignant lesions. In most cases of palpable tumors, the differentiation between benign and malignant tumors is not possible by only performing a clinical examination (4).

The many histological types of parotid neoplastic lesions make them a major challenge for radiologists and clinicians. This range of differential diagnoses influences not only the prognosis but also the treatment. Local excision or superficial parotidectomy are considered the surgical procedure of choice for patients with benign parotid tumors, in contrast to total parotidectomy in case of malignant parotid tumors. Total parotidectomy is a more difficult procedure and has the risk of facial nerve palsy (4).

In general, imaging modalities for the parotid gland include plain radiography, sialography [either conventional, computed tomography (CT), or magnetic resonance imaging (MRI), ultrasonography (US), CT, MRI, and radionuclide scintigraphy (5).

Magnetic Resonance imaging is a noninvasive technique that provides morphological information of the parotid glands and differentiates focal involvement of the gland from diffuse involvement, thus allowing a correct diagnosis to be made and proper staging in case of parotid tumors (6). Additionally, diffusion-weighted imaging (DWI) and apparent diffusion coefficients (ADCs) depend on the composition of the parotid gland as well as the different histological types of the parotid tumors. These have been reported as helpful tools for narrowing the differential diagnosis, particularly in case of parotid masses (7).

The purpose of this study was an attempt to characterize the composition of the parotid gland with diffusion-weighted echo planar imaging (DW-EPI) and to measure ADCs to depict early focal or diffuse changes in the parotid glands with differentiation between inflammatory and neoplastic lesions as well as the differentiation of the various entities of parotid gland tumors.

MATERIALS AND METHODS

This prospective descriptive analytic study was approved by the national cancer institute review board as well as the national cancer institute ethical committee, Cairo University. This study included 73 (30 male and 43 female) patients. Patients' ages ranged from 1-82 years with a mean age of 33.14±22.40 years (mean±SD). All the patients presented to our hospital (the National Cancer Institute) between July 2014 and January 2016.

Comprehensive explanations of the procedures were done for all cases including the associated risks and contraindications. Then informed consent was obtained from each patient/patient's parents in case of minor.

Technique conventional MRI

All patients were evaluated by MRI technique using 1.5 Tesla superconducting magnetic resonance imager (Achieva, Philips, Best, Netherlands). All the cases were examined in the supine position with standard circularly polarized head coil using the following sequences and parameters: axial T1WI spin echo (repetition time ms/echo time ms 659/12 ms, 256×256 matrix, 3 mm section thickness, 280 mm field of view, one signal acquired). Axial T2WI spin echo (repetition time ms/echo time ms 3680/93 ms, 256×256 matrix, 3 mm section thickness, 280 mm field of view, one signal acquired). Axial STIR (repetition time ms/echo time ms/inversion time ms 9000/116/2500 ms, 256×256 matrix, 3 mm section thickness, 280 mm field of view, one signal acquired). Coronal T1WI spin echo repetition time ms/echo time ms 430/10 ms, 256×256 matrix, 4 mm section thickness, 340 mm field of view, one signal acquired). Coronal T2WI spin echo (repetition time ms/echo time ms 3680/93 ms, 256×256 matrix, 4 mm section thickness, 340 mm field of view, one signal acquired). After intravenous administration of Gadolinium-DTPA (0.3 mg/kg), contrast enhanced T1WI (repetition time, 693 ms; echo time, 12 ms) in axial±fat suppression, sagittal and coronal planes were obtained.

Magnetic resonance DWI:

An axial EPI-DWI sequence was performed with the following parameters (repetition time, 1500 ms; echo time, 77 ms, 119×128 matrix, field of view of 250×250 mm (pixel size, 2.10×1.95 mm), six excitations, and section thickness of 5 mm with an intersection gap of 1 mm). A parallel imaging technique with an acceleration factor of 2 with 12 additional lines (modified sensitivity encoding) for self-calibrating was applied. A bandwidth of 1502 Hz/pixel was used and 12 sections were acquired. The b-factors used were 0 s/mm^2, 500 s/mm^2, and 1000 s/mm^2. Placing the frequency-selective radio-frequency pulse before the pulse sequence allowed fat suppression to be achieved. The total acquisition time of this sequence was 1 min 14 s. For each epi DWI sequence, a pixel-by-pixel ADC map was automatically calculated with the gray value of the pixel linearly corresponding to the ADC expressed in square millimeters per second.

Histopathologic analysis

Pathologic analysis of samples of parotid lesions was performed in the Pathology Department of the National Cancer Institute, Cairo University, Egypt, by a group of well-trained expert pathologists. Samples were obtained with FNAC, core biopsy, and surgical excision.

Statistical analysis

Data were statistically described in terms of mean±SD, minimum, maximum, and median. Comparison of quantitative variables between the study groups was done using Student's t-test for independent samples.

For comparing categorical data, the chi-square (χ^2) test was performed. The exact test was used instead when the expected frequency is less than 5.

Accuracy was represented using the terms sensitivity, specificity, positive predictive value, and negative predictive value.

Receiver operator characteristic (ROC) analysis was used to determine the optimum cut-off value for the studied diagnostic markers. A probability value (p-value) less than 0.05 was considered statistically significant.

The data analysis was performed using the Statistical Package for the Social Sciences (SPSS) 19.0 version (IBM Corp.; Armonk, NY, USA)

RESULTS

Locations of the lesions

Parotid lesions were classified as follows: 47.9% of the lesions were found in the right parotid gland, 45.3% were found in the left parotid gland, and 6.8% were found bilaterally in both parotid glands. Of the studied lesions, 17.9% were found in the deep lobe, 47.9% were found in the superficial lobe, and 34.2% were found in both lobes.

Pathological diagnosis

Patients were distributed according to their final pathological diagnosis into three groups: inflammatory lesion group, benign tumor group, and malignan tumor group. The inflammatory lesion group included 7 patients, the benign tumor group included 23 patients, and the malignant tumor group included 43 patients.

The diagnoses in the benign tumor group as determined by performing a pathological analysis were diverse: pleomorphic adenoma, Warthin's tumor, hemangioma, lymphangioma, basal cell adenoma, and others. Pleomorphic adenomas were the most frequent among benign lesions and represented 43.34% of all benign lesions.

The patients in the malignant group showed the following entities: mucoepidermoid carcinoma, adenoid cystic carcinoma, basal cell carcinoma, mixed salivary gland tumor, rhabdomyosarcoma, lymphoma, leukemic infiltrates, metastatic intra-parotid lesions, and others. Even rare pathological types were found such as primitive neuroectodermal tumor (PNET).

The most common malignant lesions found in our study were metastatic lesions in the parotid gland (i.e., direct infiltration or distant metastasis) that represented 30.23% of all malignant lesions, while the most common primary parotid tumor was found to be adenoid cystic carcinomas that represented approximately 18.6% of all malignant lesions.

Conventional MRI

The normal parotid glands were comparable on both sides showing equal size and symmetrical smooth regular contours. A little difference was noted along the gland among variable age groups relative to the increase fat content with age. On the basis of signal criteria and contrast uptake, the normal parotid glands appeared heterogeneously high on T1WIs with a diffuse signal drop in STIR & fat suppression techniques and relatively high T2WIs "relative to muscles" owing to high fat content of the gland. The glands enhance smoothly after contrast administration like muscles. Regarding T1WI signals, 57 lesions had low signal intensity, 12 lesions had intermediate signal intensity, and 4 lesions had high signal intensity. Regarding T2WI signals, 4 lesions had low signal intensity, 13 lesions had intermediate signal intensity, and 55 lesions had high signal intensity. The enhancement pattern was studied, and it was found that 2 lesions display no enhancement, 28 lesions displayed homogenous enhancement, and that the remaining 43 lesions displayed heterogeneous enhancement.

When the lesions were assessed regarding their margins; 45 lesions (61.6%) were well defined and the remaining 28 lesions (38.4%) showed ill-defined borders. While assessing relationship of the lesions to surroundings; 25 lesions (34.2%) showed vascular encasement, 20 lesions (27.4%) showed facial nerve involvement, 10 lesions showed perineural spread "8 lesions (10.96%) through facial nerve and the remaining 2 lesions (2.74%) via the auriculotemporal nerve branch of mandibular division of the trigeminal nerve", 2 lesions (2.74%) showed intracranial extension and 3 lesions (4.1%) were aggressive and showed bone invasion. Regarding the presence of lymph nodes; 12 lesions (27.91%) showed malignant looking lymph nodes nodes, 10 lesions (31.5%) were associated with bilateral subcentimetric lymph nodes likely reactive, and 41 lesions had no associated enlarged lymph nodes.

Accuracy of conventional MRI

Lesions were assessed primarily with conventional MRI alone. They were labelled as either benign-looking (B) or malignant-looking (M), according to presence of criteria of malignancy; e.g. ill-definition of margins, invasion of the surrounding tissues or presence of suspicious-looking lymph nodes.

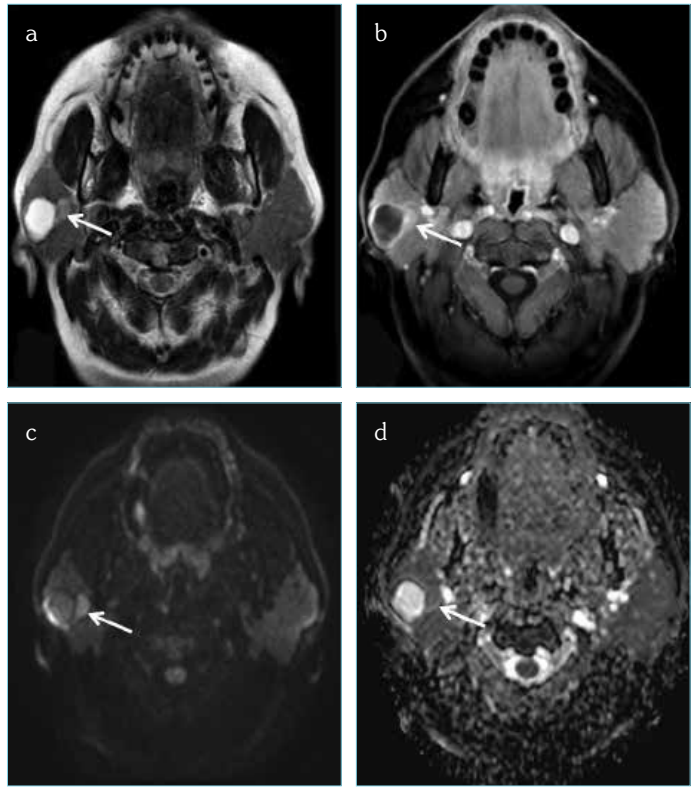

Figure 1. a-d. MRI of 43 year old female presented with right parotid welling. Axial T2 weighted MR image (a), contrast enhanced T1 with fat suppression (b), DWI (c) and ADC map showed (d); Well circumscribed lesion with peripheral nodular enhancing soft tissue component "white arrow" is seen involving the superficial lobe of the right parotid gland. The lesion displays high T2 signal and irregular peripheral enhancement in the post contrast series. Large non enhancing central area of fluid signal is seen representing area of breaking down. The irregular nodular peripheral enhancing area "white arrow" appears high in DWI and low in ADC map denting restricted diffusion pattern, while the non-enhancing central portion shows high signal in DWI and ADC map denoting T2 shine through. ADC value measures: $0.756x10^{-3}$ mm^2/sec. Pathological evaluation revealed mixed salivary tumor "carcinoma ex-pleomorphic adenoma"

By conventional MRI alone, 47 malignant-looking lesions were detected, when they were compared to the pathology results; only 32 proved to be truly positive for malignancy with the remaining 15 lesions were false positive cases. Twenty-five lesions were benign-looking also when these were compared to the pathology results; only 15 lesions were truly negative for malignancy with the remaining 10 lesions were false-negative ones.

Thus, using conventional MRI alone in predicting benign and malignant lesions has a sensitivity of 76.19% [95% confidence interval (CI), 60.55-87.95%] and specificity of 50% (95% CI, 31.30-68.70%) with a positive predictive value of 68.09% (95% CI, 52.88-80.91%) and negative predicative value of 60% (95% CI, 38.67-78.87%). The positive and negative likelihood ratios were 1.52 and 0.48, respectively.

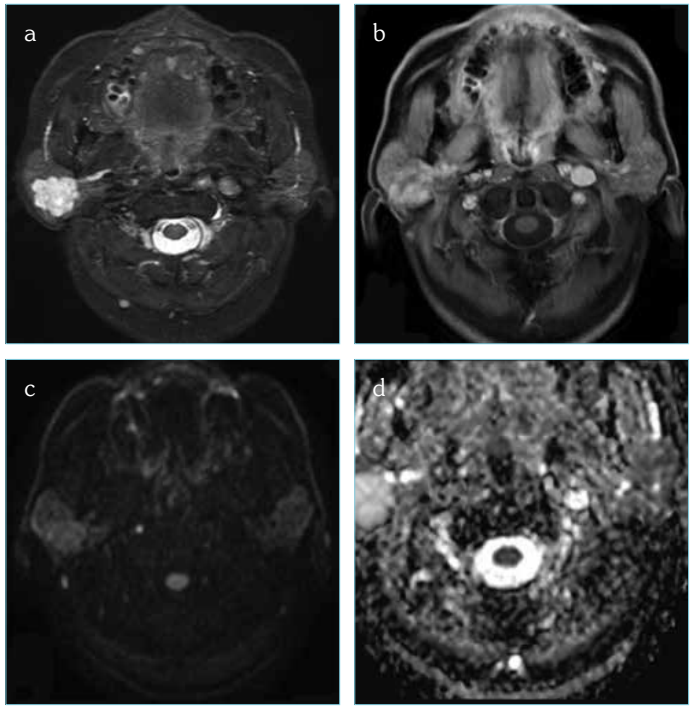

Figure 2. a-d. MRI of 59-year-old male presented with right parotid welling. Axial short tau inversion recovery "STIR" images (a), contrast enhanced T1 with fat suppression (b), DWI (c) and ADC map showed (d); Right parotid deep lobe lobulated soft tissue lesion is seen displaying and high STIR signal with heterogeneous enhancement in the post contrast series. The lesion shows high signal in DWI and ADC map denoting "T2 shine through". ADC value measures: 1.832x10^{-3} mm^2/sec. This lesion is found to be pleomorphic adenoma on histopathology

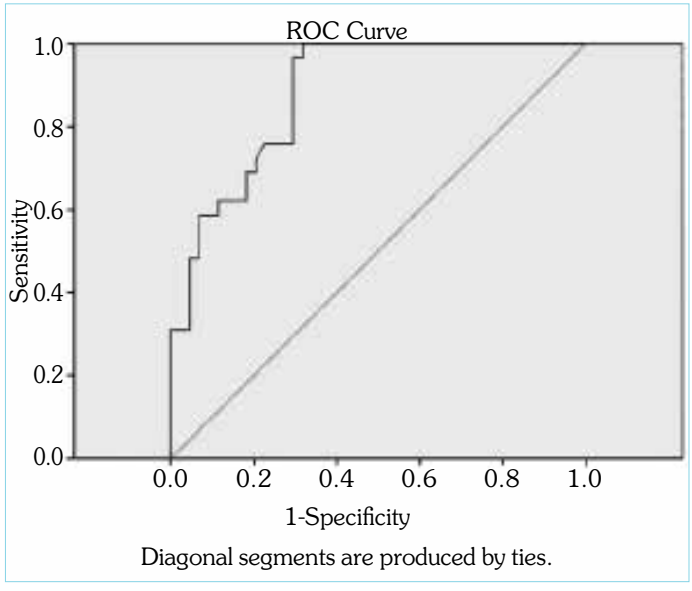

Figure 3. Shows the probability of ADC in differentiation between benign and malignant lesions

DWI qualitative analysis of DWIs "signal intensity"

Normal parotid glands showed diffuse homogenous low signal intensity on performing DWI. The signal intensity of the benign tumor and malignant groups in diffusion-weighted images was visually assessed as having two levels of varying intensity.

A significant difference was found between the benign and malignant tumor groups as approximately 90.7% of all malignant lesions displayed hyper-intense signal intensity (SI) in DWI "represent restricted diffusion pattern" (Figure 1), while 86.7% of the benign lesions showed lesser signal intensities "represent facilitated diffusion pattern" (Fig. 2).

Table 1. Mean ADCs, standard deviation, minimum and the maximum Values of the different lobes of the normal parotid glands adcs:

Site of the gland	Mean	SD	Minimum	Maximum
Rt superficial lobe	0.89	0.2	0.4	1.48
Rt deep lobe	1.02	0.27	0.49	1.92
Lt superficial lobe	0.9	0.17	0.51	1.34
Rt deep lobe	0.97	0.16	0.68	1.42

ADCs: apparent diffusion coefficients; SD: standard deviation

Table 2. Mean ADC, SD, median, minimum and maxmum values of the normal parotid glands. adcs: apparent diffusion coefficients

	Mean	Standard Deviation	Median	Minimum	Maximum
ADC	1.123	0.121	0.914	0.396	1.924

ADC: apparent diffusion coefficient; SD: standard deviation

Quantitative analysis of DWIs "ADC "

Apparent Diffusion Coefficients for normal parotid glands were obtained for the superficial and deep lobes on both sides and showed different values as shown in Table 1.

When these results modified for the whole gland showed a mean ADC of 1.123×10^{-2} mm^2/s and SD of±0.121x10^{-3} (95% CI, 1.0954-1.1506). Table 2 shows the mean, SD, and median of the ADCs of normal parotid glands.

Apparent Diffusion Coefficients were calculated in the solid component of all lesions. The calculated ADCs ranged from 0.3×10^{-3} to 2.4×10^{-3} mm^2/s (mean±SD=0.96×10^{-3}±0.42×10^{-3} mm^2/s).

The calculated ADC of the lesions was found to be statically significant in the differentiation between inflammatory and neoplastic conditions as well as in the differentiation between benign and malignant lesions. The mean±SD ADC in inflammatory conditions was 0.86×10^{-3}±0.3×10^{-3} mm^2/s, and the mean ADC±SD in benign lesions was 1.16×10^{-3} ±0.31×10^{-3}mm^2/s. The mean ADC in malignant lesions was 0.82×10^{-3}±0.11 x 10^{-3}mm^2/s (p-value less than 0.001). The mean ADC in lesions containing myxoid matrix such as pleomorphic adenoma was found to be 1.3×10^{-3}±0.71x10^{-3}mm^2/s.

The diverse pathologies detected in our study made the comparison between different types in an attempt to attribute suggestive

ADCs for each type quite difficult. Further studies dedicated to these subtypes separately may be of further value in comparing them.

Accuracy of DWI

Lesions were assessed with DWI alone. They were labelled as either benign-looking (B) or malignant-looking (M), according to presence of criteria of malignancy; e.g. high signal in DWIs "i.e. restricted diffusion pattern" and low ADC.

By diffusion-weighted imaging alone, 44 malignant-looking lesions were detected after the pathological analysis; only 39 lesions were truly positive for malignancy, with 5 false-positive cases. Twenty-nine lesions were detected as benign-looking; only 25 were truly negative for malignancy, with 4 false-negative cases.

Thus, the use of DWI alone in predicting benign and malignant lesions had a sensitivity of 90.70% (95% CI, 77.86-97.41%) and specificity of 83.33% (95% CI, 65.28-94.36%) with a positive predictive value of 88.64% (95% CI, 75.44-96.21%) and negative predicative value of 86.21% (95% CI, 68.34-96.11%). The positive and negative likelihood ratios were 5.44 and 0.11, respectively.

Accuracy of conventional MRI when combined with DWI

The lesions were assessed again by combining conventional MRI findings with DWI and the DWI signal intensity and ADC.

After the combination of conventional MRI and DWI, 43 malignant-looking lesions were detected; 42 were true malignant lesions, with one false-positive case. Thirty benign-looking lesions were detected; 29 were positive, with one false-negative cases.

Thus, combining DWI and ADCs increased the accuracy as the sensitivity and specificity were 97.67% (95% CI, 87.71-99.94%) and 96.67% (95% CI, 82.78-99.92%), respectively, with a positive predictive value of 97.67% (95% CI, 87.71-99.94%) and negative predicative value of 96.67% (95% CI, 82.78-99.92%).

Logistic regression and ROC curve analysis were performed to determine the cut-off value between benign and malignant lesions (Figure 3). The absolute and relative ADCs of lesions had significant probability in the characterization between benign and malignant lesions.

ADC value of 0.93×10^{-3} mm^2/s was set as cut-off value for benign and malignant parotid tumors with sensitivity and specificity of 72.09% and 82% for ADC respectively.

DISCUSSION

Parotid gland has diverse spectrum of pathological conditions that could be focal or diffuse being unilateral or bilateral. Differentiation between inflammatory or neoplastic lesions could be suspected clinically; however, more accurate differentiation requires multimodality imaging and in some cases FNAC. Parotid gland tumors can be often diagnosed by FNAC, yet these minimally invasive procedures entail the risk of tumor spillage and inconclusive results owing to insufficient samples for histopathological analyses. Thus, preoperative imaging plays an important role in the evaluation of tumor characteristics (8).

Magnetic resonance imaging is a non-invasive procedure that could accurately depict abnormalities within the parotid glands depending upon the morphological criteria such as size, margin, signal, and enhancement pattern.

The potential additional value of diffusion in imaging lies in the fact that it provides functional tissue information, which can be combined with anatomical magnetic resonance images to improve the specificity of lesion characterization. The DWI studies and ADC measurements provide useful information about the cellularity of the gland, potential inflammatory or neoplastic changes in its composition and moreover tumor cellularity that can correlate with its histological pattern and give a clue in the differentiation between benign and malignant tumors (8).

Thus, this work aimed to study the value of DWI and ADC measurement coupled with high-resolution MRI in effective characterization of normal parotid glands and thus might be valuable in the detection of early pathological conditions as well as differentiation between inflammatory and neoplastic lesions. We also expected that ADC mapping would differentiate benign and malignant tumors.

The mean ADC of the normal parotid gland was found to be $1.12\times10^{-3}\pm0.12\times10^{-3}mm^2/s$. This is comparable with the findings of Alifa et al. (9) who reported in 2012 that the mean ADC of normal parotid tissue was $1.04\times10^{-3}\pm0.13\times10^{-3}$ mm^2/s.

Juan et al. (10) showed in 2009 that the mean ADC for normal parotid tissue was $1.08810^{-3}\pm0.12\times10^{-3}$ mm^2/s. There are some factors that distort ADC measurement: susceptibility-related image distortion and the parotid fat content.

The Apparent Diffusion Coefficient matches to tumor cellularity and the characteristics of extracellular components. Parotid gland tumors are histopathologically unique in terms of extracellular components such as myxoid matrix (e.g., pleomorphic adenoma).

In our study, the tumors with myxoid matrix such as pleomorphic adenoma showed high ADCs with a mean value of $1.3\times10^{-3}mm^2/s$. These results are comparable with the results obtained in previous studies such as those by Matsushima et al. (8), who tested parotid tumors with myxoid and chondroid matrices e.g., pleomorphic adenoma, neurofibroma and myxoid liposarcoma, this showed high ADCs with a mean ADC of 1.5×10^{-3} mm^2/s.

We found that the mean±SD ADC for benign tumors was $1.16\times10^{-3}\pm0.31\times10^{-3}$ mm^2/s. These values were lower than the results published by Alifa et al. (9) who stated the mean ADC±SD for benign tumors was $1.91\times10^{-3}\pm0.45\times10^{-3}$ mm^2/s.

In our study, the mean ADC for malignant tumors found to be 0.82×10^{-3} mm^2/s. These results were comparable to the results by Matsushima et al. (8) who found that the mean±SD ADC for malignant tumors was $1.09\times10^{-3}\pm0.34\times10^{-3}$ mm^2/s, Lechner et al. (11) found that the mean±SD ADC for malignant tumors was $0.83\times10^{-3}\pm0.16\times10^{-3}$ mm^2/s and Alifa et al. (9) reported that the mean±SD ADC for malignant tumors was $1\times10^{-3}\pm0.37\times10^{-3}$ mm^2/s. These results also were slightly lower than the values previously published (e.g., $1.19\times10^{-3}\pm0.19\times10^{-3}$ mm^2/s by Ikeda et al. (12) and $1.13\times10^{-3}\pm0.43\times10^{-3}$ mm^2/s by Wang et al. (13).

The cut-off value of the ADC, below which a parotid tumor is suggestive of being malignant, were set to 0.93×10^{-3} mm^2/s. This was found to be lower than that obtained in previous studies (i.e., Lechner et al. (11) who found the cut-off value to be 1.22×10^{-3} mm^2/s).

CONCLUSION

The present study showed that ADC measurement has the potential to depict early pathological changes in the parotid glands, differentiate between inflammatory and neoplastic conditions, and differentiate between benign and malignant focal parotid lesions.

The obtained results for determining whether a parotid gland tumor is benign or malignant based on combining morphologic features and DWI and ADC measurements in a diagnostic noninvasive approach are very promising and might decrease the number of unnecessary invasive procedures (e.g., biopsies or inappropriate extensive surgical approaches for benign parotid lesions). This is particularly promising for the differentiation of pleomorphic adenomas and Warthin's tumors as well as carcinomas.

Some limitations to this study can be contributed to the small sample size, the diverse spectrum of the pathological conditions of the parotid glands, and the high dependence on neoplastic lesions. Therefore, further studies should be conducted to make a more solid base in the value of ADC measurement, hence accurate cut-off value, in the early detection of parotid pathological changes and to discriminate between benign and malignant parotid neoplastic lesions.

We recommend adding DWI in the MRI protocol for the detection as well as qualitative and quantitative discrimination of parotid neoplastic lesions.

Ethics Committee Approval: Ethics committee approval was received for this study from the ethics committee of the National Cancer Institute, Cairo University.

Informed Consent: Written informed consent was obtained from patients who participated in this study.

Peer-review: Externally peer-reviewed.

Author Contributions: Conceived and designed the experiments or case: AN. Performed the experiments or case: AN. Analyzed the data: AY., AEB. Wrote the paper: AN. All authors have read and approved the final manuscript.

Conflict of Interest: No conflict of interest was declared by all authors.

Financial Disclosure: The authors declared that this study has received no financial support.

REFERENCES

1. Yousem D., Krout M. and Chalian A. Major salivary gland imaging. Radiology 2000; 216(1): 19 -29. [CrossRef]
2. Gadodia A, Bhalla AS, Sharma R, Thakar A, Parshad R. Bilateral parotid swelling: A radiological review. Dentomaxillofac Radiol 2011 40(7): 403-14. [CrossRef]
3. Howlett DC, Kesse KW, Hughes DV, Sallomi DF. The role of imaging in the evaluation of parotid disease. Clin Radiol 2002; 57(8): 692-701. [CrossRef]
4. Thoeny H. Imaging of salivary gland tumours. Cancer Imaging 2007; 7(1): 52 - 62. [CrossRef]
5. Rastogi R, Bhargava S, Mallarajapatna GJ, Singh SK. Pictorial essay: Salivary gland imaging. Indian J Radiol Imaging 2012; 22(4): 325-33. [CrossRef]
6. Yerli H, Aydin E, Haberal N, Harman A, Kaskati T, Alibek S. Diagnosing common parotid tumors with magnetic resonance imaging including diffusion-weighted imaging vs. fine-needle aspiration cytology: a comparative study. Dentomaxillofac Radiol 2010; 39(6): 349-55. [CrossRef]
7. Motoori K, Iida Y, Nagai Y, Yamamoto S, Ueda T, Funatsu H, Ito H, Yoshitaka O. MR imaging of salivary duct carcinoma. AJNR Am J Neuroradiol 2005; 26(5): 1201-6.
8. Matsushima N, Maeda M, Takamura M, Takeda K. Apparent diffusion coefficients of benign and malignant salivary gland tumors. Comparison to histopathological findings. J Neuroradiol 2007; 34(3): 183-9. [CrossRef]
9. Alifa D, Khaled B, Kalil K, Chiraz JC, Lamia RM, Mohamed habib D, et al. Utility of diffusion-weighted MRI in distinguishing benign and malignant parotid lesions. ECR 2012/ C-2619.
10. Juan C, Chang H, Hsueh C, Liu H, Huang Y, Chung H, et al. Salivary Glands: Echo-Planar versus PROPELLER Diffusion weighted MR Imaging for Assessment of ADCs. Radiology 2009; 253 (1): 144-52. [CrossRef]
11. Lechner Goyault J, Riehm S, Neuville A, Gentine A, Veillon F. Interest of diffusion-weighted and gadolinium-enhanced dynamic MR sequences for the diagnosis of parotid gland tumors. J Neuroradiol May 2011; 38(2): 77-89. [CrossRef]
12. Ikeda M, Motoori K, Hanazawa T, Nagai Y, Yamamoto S, Ueda T, et al. Warthin tumor of the parotid gland: diagnostic value of MR imaging with histopathologic correlation. Am J Neuroradiol 2004; 25(7): 1256-62.
13. Wang J, Takashima S, Takayama F, Kawakami S, Saito A, Matsushita T, et al. Head and neck lesions: characterization with diffusion-weighted echo-planar MR imaging. Radiology 2001; 220(3): 621-30.[CrossRef]